REGENERATIVE THERMOELECTRIC COOLING FOR IMPLANTABLE

MEDICAL DEVICES

An Undergraduate Research Scholars Thesis

by

SAMUEL PATTERSON

Submitted to the LAUNCH: Undergraduate Research office at
Texas A&M University
in partial fulfillment of requirements for the designation as an

UNDERGRADUATE RESEARCH SCHOLAR

Approved by
Faculty Research Advisors:

Dr. Aydin I. Karsilayan
Dr. Jose Silva-Martinez

May 2022

Major: Electrical Engineering

RESEARCH COMPLIANCE CERTIFICATION

Research activities involving the use of human subjects, vertebrate animals, and/or biohazards must be reviewed and approved by the appropriate Texas A&M University regulatory research committee (i.e., IRB, IACUC, IBC) before the activity can commence. This requirement applies to activities conducted at Texas A&M and to activities conducted at non-Texas A&M facilities or institutions. In both cases, students are responsible for working with the relevant Texas A&M research compliance program to ensure and document that all Texas A&M compliance obligations are met before the study begins.

I, Samuel Patterson, certify that all research compliance requirements related to this Undergraduate Research Scholars thesis have been addressed with my Research Faculty Advisors prior to the collection of any data used in this final thesis submission.

This project did not require approval from the Texas A&M University Research Compliance & Biosafety office.

TABLE OF CONTENTS

ABSTRACT

Regenerative Thermoelectric Cooling for Implantable Medical Devices

Samuel Patterson
Department of Electrical and Computer Engineering
Texas A&M University

Research Faculty Advisor: Dr. Aydin I. Karsilayan
Department of Electrical and Computer Engineering
Texas A&M University

Research Faculty Advisor: Dr. Jose Silva-Martinez
Department of Electrical and Computer Engineering
Texas A&M University

Implantable Medical Devices (IMDs) are a category of medical devices that include pacemakers, implantable cardiac defibrillators, spinal cord stimulators, and many other devices. Many of these devices are battery-powered such as pacemakers which last an average of 7 years before needing to be replaced via surgery. This research focuses on re-chargeable IMD's such as spinal cord stimulators. Re-chargeable IMD's often require daily charging to operate which can be a burden on the patient. Shorter charge times are desired for improved usability. One significant limitation of these re-chargeable IMD's is that the charging current is reduced from optimal levels to mitigate heat buildup of the device. A high heat generation during charging is not acceptable due to FDA regulations that IMD's are bound by. This heat is primarily emitted from the charging battery-element within the IMD and can be harmful to human patients. Unfortunately, limiting the

current throughput as a solution for the generated heat, results in a longer charging time that affects a patient's quality of life.

This paper serves to document the research performed on the integration of thermoelectric generators (TEGs) in such medical devices. It will present the thermal impacts that a TEG has when operating under similar conditions as an IMD. The TEG serves to harvest the heat energy that is normally wasted by the battery and convert it into electrical energy. The conversion from heat into electrical energy serves as a cooling mechanism for the system that correlates with the resulting charging times of IMD's. A maximized cooling effect implemented by the TEG will further reduced IMD charging times. The mitigation of heat being introduced to the system will allow for increased charge current to be safely introduced, further increasing the rate of charge. This research will explore how effective thermoelectric devices can be in reducing the charge time for these medical devices. Ultimately, this research aims to increase the quality of life for IMD patients by addressing the thermal obstacle present in these devices.

ACKNOWLEDGEMENTS

NOMENCLATURE

IMD	Implantable Medical Device
TEG	Thermoelectric Generator
FDA	Food and Drug Administration
Ft	Feet
°F	Degrees Fahrenheit
°C	Degrees Celsius
W/m*k	Watts per meter-kelvin
MPPT	Maximum Power Transfer
CPU	Central Processing Unit of a computer
mm	Millimeters
'	Inches
MOSFET	Metal-oxide-semiconductor field-effect transistor
Ω	ohms of resistance
µF	microfarads of capacitance
mH	millihenries of inductance
Hz	Units of frequency in Hertz
AD2	Analog Discovery 2 – USB oscilloscope and logic analyzer
DC	Direct Current

1. INTRODUCTION

1.1 Background

The vast majority of Implantable Medical Devices (IMDs) are powered by non-rechargeable batteries that last, on average, 5-7 years before needing to be replaced. It is common practice to replace the entire device rather than attempting to change battery itself. This has the benefit of a patient receiving a new, and likely improved, IMD to replace their old one. Unfortunately, when device's battery gets close to depletion, the patient must undergo surgery to replace the device. Thus, every 5-7 years, a patient will go back in for surgery.

Rechargeable IMD's have the benefit of eliminating the need for surgery at the expense of needing to recharge the device. Additionally, some implantable devices require much more energy to function and thus, depend upon rechargeable platforms. One such device is called a spinal cord stimulator. These devices are used to help patients that experience chronic pain by introducing an electric current into their nervous system. These devices must be charged daily to ensure their operation. Charge time of the device is one of the primary factors in the patient's quality of life. The charging times are currently limited by the resultant heat buildup of the device during charging. This heat can pose a health risk to the patient and is one parameter that is strictly regulated by the FDA. The only solution has been to limit the current throughput to the device. While this does mitigate the heat generation from the battery, it also reduces the charging rate of the device. Thus, the only way to make charging easier for the patients is to address the battery's thermal output.

1.2 Overview

Traditional cooling mechanism's include the use of fans or liquid-cooling to dissipate the heat by quickly transfering it away from the heating source. A great example of this is the CPU in a computer. The CPU's heat output is managed by transfering the thermal energy out of the computer and bringing in the colder air from the external environment. Unfortunatley, such techniques cannot be leveraged for IMD's since they operate inside the human body. By operating in an enclosed environment, simple heat dissipation is not possible. This makes energy harvesting a more appealing solution to leverage. Rather than wasting the heat energy by transferring it away from the system, energy harvesting re-captures the energy and often converts it into another form. Much like the way regenerative braking in car's can re-capture the kinetic energy of the car to charge the battery, the IMD's thermal output can be harvested within the enclosed environment that it operates in. Thermoelectric devices allow for conversion between thermal energy and electrical energy.

This research project aims to minimize the heat buildup of IMD's during the charging process without sacrificing current throughput. An imbedded Thermoelectric Generator (TEG) will convert some of the heat energy into electrical energy. The TEG will only function during the charging process as it requires a sufficient heat gradient to operate. When the internal temperature is the same as or lower than the external temperature, the system will shut down. The generation of electrical energy corresponds to an equal reduction of heat energy. The conversion of energy will introduce a cooling effect on the system.

1.3 Objectives

Heat generation from an IMD's battery is challenging to deal with because these devices operate in enclosed environments. Solid-State devices, such as TEG's, are perfectly suited to

address the issue. This research will focus solely on the impacts that thermoelectric devices can make on the system. Since the IMD's thermal output is the primary limiting factor affecting the devices charging times, this will the focus for this project. I will design a system that replicates an IMD's operating conditions. The system must include a heating element representing the heating battery. I will then design a system that uses TEGs to harvest the thermal energy and convert as much as possible into electrical energy. By maximizing the conversion efficiency of my overall thermoelectric design, I can maximize the cooling effect on the system. A maximized cooling potential will demonstrate how effective a TEG can improve IMD charging rates.

It does not make sense to simply convert into electrical energy without having a use for that energy. There are two logical options to choose from. The first option is to try to use that electrical energy to further enhance the cooling capability of the system. This is something that was explored and determined to be ineffective within the enclosed environment of an IMD. The second option is further charging the IMD's battery. This will require the use of a boost converter to boost the low output voltage of the TEG to a more usable level. Since the first option is not feasible, the electrical energy output from the harvesting circuit will ultimately be used to charge a battery or capacitor.

2. PROPOSED SYSTEM FOR IMD THERMOELECTRIC COOLING

2.1 Project Scope

The thermoelectrically cooled IMD will improve patient quality of life by reducing the charging time required. When a patient begins to recharge their IMD, the internals will begin to heat, much like in a laptop or phone. When the temperature gradient between the internals of the device and the exterior forms, the TEG will turn on and begin to convert that heat into electricity.

I do not have access to an IMD to be used for testing. Additionally, I do not have the resources to implement a design small enough to be embedded in an IMD. Thus, my project design will replicate the conditions present in the IMD device. Most notably, a heating element will be used to represent the IMD battery. A power harvesting circuit will then be constructed that makes use of thermoelectric devices to convert as much thermal energy as possible into electrical energy. This electrical energy will serve as the input to a low-voltage boot strap boost converter to sufficiently charge a capacitor or battery. Upon integration of the heating element with the power harvesting circuit, the temperature readings of the TEG and voltage output of the boost converter will be recorded.

In the final phase of this research project, the commercial boost converter that was originally implemented will be switched out for my own boost converter design. This boost converter will be comprised of discrete components on a breadboard used to boost the ultra-low TEG voltage higher. With this new design, voltage and temperature readings will be re-recorded and compared with the initial findings.

2.2   System Overview

The focus of this project is to utilize TEG technology to enable faster charging rates for Implantable Medical Devices. This will be accomplished by reducing the internal temperature of the IMD. The Thermoelectrically Cooled IMD will be comprised of five subsystems. The five subsystems include: Thermoelectric Generator, DC-DC Boost Converter, Heating Element, Measurement Equipment, and Body-Representative Medium. The primary sub-systems are connected as depicted in Figure 2.1.
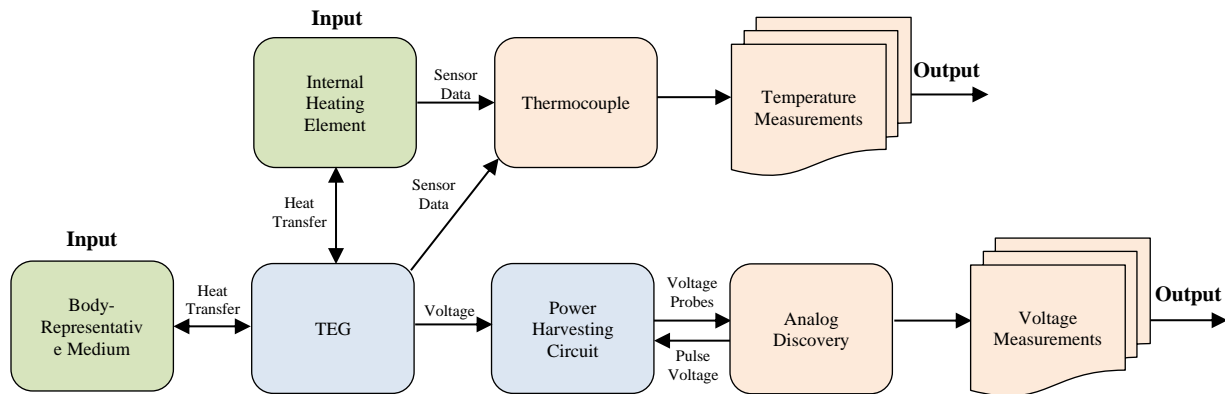

Figure 2.1: System Block Diagram

The input to the system will be the heat that is emitted from the heating element. That thermal energy is fed directly into the TEG to be converted into electrical energy. If possible, a material with similar thermal characteristics as the human body will be interfaced on the external plate of the TEG. A medium such as water would imitate the human body with relative accuracy. When integrated with the system, the selected medium will replicate the enclosed environment that IMDs operate in. The output from the TEG will be fed into the power harvesting circuit which is comprised of a DC-DC boost converter. The boost converter will boost the output from the TEG (a few hundred millivolts) to at least 1.5 V. The output voltage from the boost converter will depend on the load as well as the design parameters chosen for the converter. During the

experiment, an analog discovery will be used to measure the voltage output from the system as well as provide the required pulse input for the boost converter. A thermocouple will be used to measure the temperature of the external face of the TEG. An additional TEG will be present during the experiment and interfaced with the heating element however, it will be in an open circuit configuration. This will ensure that it is inactive and can be used as a baseline comparison against the active TEG that is connected to the system.

2.3   Sub-System Details

The final design will be composed of the following systems:

- A thermoelectric generator

- A DC-DC Boost Converter

- A heating element

- Body-representative medium

- Measurement equipment

2.3.1   Thermoelectric Generator

A Thermoelectric generator (TEG) is a solid-state device that converts between thermal and electrical energies. This is accomplished using two metal plates separated by n and p-type thermoelements, as shown in Figure 2.2 [1]. When a temperature gradient is induced between its two plates, a voltage can be observed at its output. The output voltage has a magnitude that is proportional to the temperature gradient across the two plates. The voltage produced from a device operating on the Seebeck effect is given by:

$$V_{oc} = j \times S \times \Delta T \tag{2.1}$$

where j is the number of series connected elements, S is the Seebeck coefficient, and ΔT is the temperature gradient applied [2].
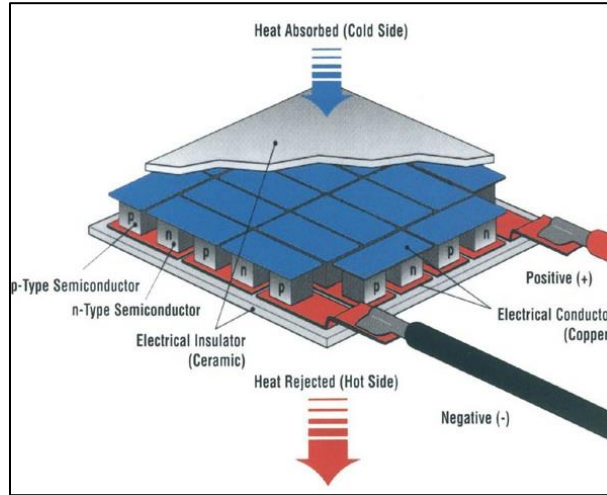

Figure 2.2: Thermoelectric Generator (Reprinted from [1])

The selected TEG is a TXL-287-03Z module from TXL Group. This is a 2.44' by 2.44' Bismuth Telluride module that is comprised of 287 thermoelectric couples with an internal resistance of 8.3Ω. It is rated up to a maximum of 125°C and has a Seebeck coefficient of

$$S = 200 \frac{\mu V}{°C} \tag{2.2}$$

at room temperature increasing at 0.4% per degree C with temperature rise [3]. This allows for easy approximation of the open circuit voltage as

$$V_{oc} = 574 \times (0.0002 \times 1.004^{\varDelta T}) \times \varDelta T \tag{2.3}$$

where ΔT is the temperature gradient between the two plates [3]. In my design, the temperature gradient between the heating element and the external environment will produce the voltage output. As mentioned previously, using a medium such as water for the external plate will best replicate a real IMD.

TEG's are preferred over standard Peltier devices since they are optimized for voltage generation which uses the Seebeck effect. This will ensure that cooling can be better prioritized. Both will have their hot faces interfaced with the heating element however only one will be active. The active TEG will have its voltage leads connected to the power harvesting circuit to actively transfer power to a load. The inactive one will be left in an open circuit configuration to ensure there is not transfer of power. This will allow for an accurate baseline comparison to test the effectiveness of an active TEG that is transferring from thermal power to electrical power.

2.3.1.1 Thermoelectric Generator Functional Validation

The selected TXL-287-03Z TEG module was tested to ensure proper functionality. This was done prior to integration with the other sub-systems to ensure the expected operation of the final design. The TEG's functionality and outputs were tested using a hotplate set at 65°C with the ambient room temperature as the cold side. I let the hotplate heat up to 65°C before placing the TEG hot side on top and measured the resultant open circuit voltage using an Analog Discovery. With this setup, I would expect the TEG to quickly reach a maximum open circuit output voltage as the greatest temperature difference will occur at the very beginning. As the hot side quickly heats up, I should then see the unharvested heat dissipate to the cold side and result in a smaller temperature gradient. This should then reduce the output voltage.
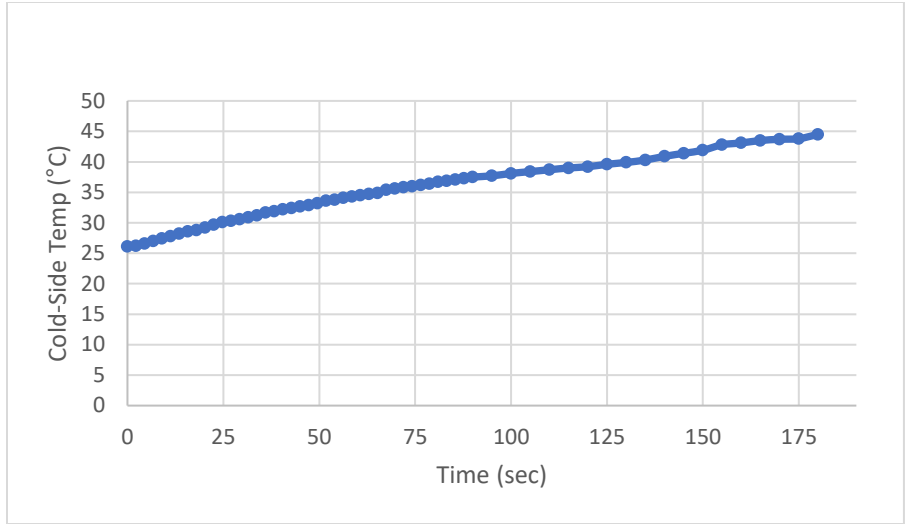
Figure 2.3: TEG Functional Test Temperature Output

Figure 2.3 reflects an observed heat rate of 5-7°C/min at the cold side of the TEG with the ΔT_{max} of 39°C. This confirms that, without a medium acting as a heatsink at the cold side of the TEG, the unconverted thermal energy begins to quickly make its way to the opposite side of the TEG. This limits the time of operation for the TEG and further stresses the importance of a body-like medium such as water at the cold side of the TEG during testing.
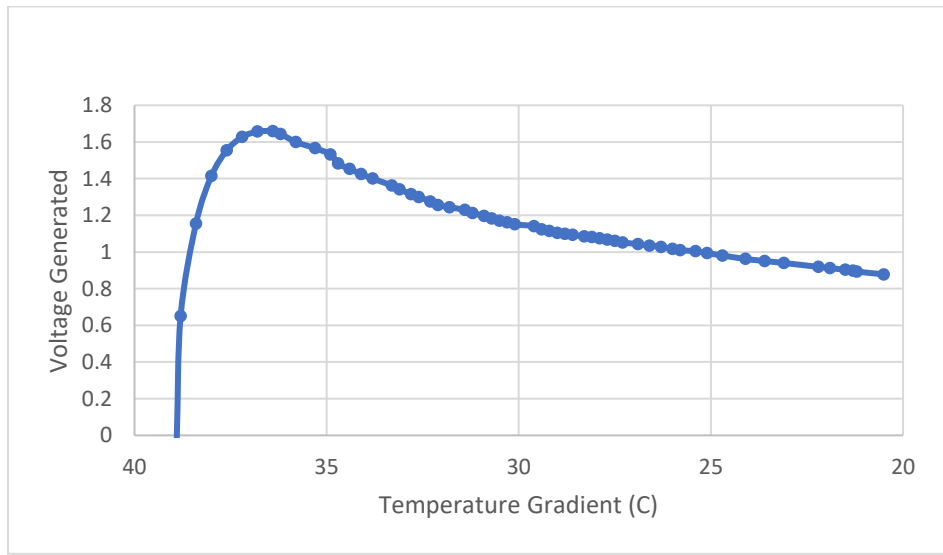

Figure 2.4: TEG Voltage vs. ΔT during Functional Test

13

The TEG output voltage depicted in Figure 2.4 confirmed my expectations. The TEG had output the greatest voltage at the beginning, when the ΔT was greatest. More importantly, I saw an output voltage of 1.65V with the corresponding ΔTmax of 39°C. The FDA limits the thermal output of an implanted device to not exceed 5°C above the body temperature. This leaves a maximum ΔT of 5° across the TEG. Thus, if applying only a 5°C across the TEG, the open circuit voltage can be calculated as:

$$V_{oc} \ at \ 5°C = 1.65 * (5/39) = 200mV \qquad (2.4)$$

This meets my minimum of 40 mV within a 5°C maximum and aligns with what the data sheet for the TEG indicated. These results indicate that my TEG's are sufficient to activate my boost converter under the specified testing conditions.

2.3.2 DC-DC Boost Converter

Thermoelectric Generators provide an output voltage in the order of a few hundred millivolts at small temperature gradients. A low voltage boost converter is essential for converting the voltage into a usable level for embedded systems. DC-DC Boosters, also known as switching regulators, are comprised of an inductor, a switching device, a diode, a capacitor, and a load. An image of a typical boost converter topology is shown below in Figure 2.5.
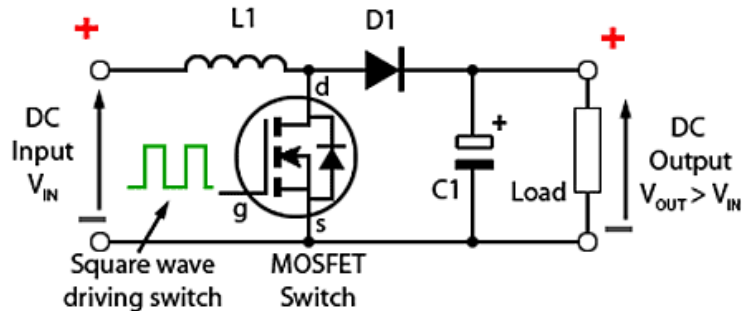

Figure 2.5: DC-DC Boost Converter Diagram (Reprinted from [4])

14

First, I will experiment using a Custom Thermoelectric bootstrap boost converter purchased commercially. The selected converter is the VB-0410-2 (gold), as depicted in Figure 2.6. This DC booster is uniquely suited for thermoelectric projects since it is designed for inputs as low as 40mV and features maximum power point tracking (MPPT) to ensure an efficient power transfer to the load [2]. Without a load, the output of the boost converter reaches ~10 V.
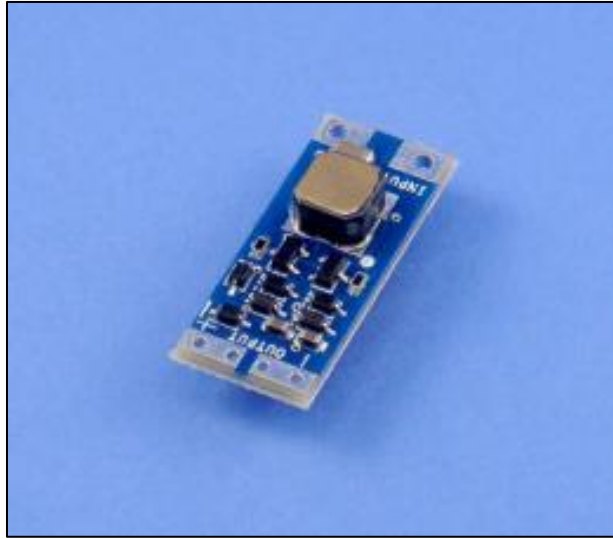

Figure 2.6: ELC-BVB040 Bipolar Voltage Booster 40mV (Reprinted from [2])

After testing with the commercial booster, a custom design will be built and implemented using discrete components. To minimize losses and ensure functionality at high switching frequencies, I must use robust and reliable components in my boost converter design. The selection of the switching device and diode is particularly important. The switch must have a minimized drain to source resistance and the diode must have a minimized forward voltage. The switch that was selected is an IRF3205 power MOSFET from International Rectifier, depicted in Figure 2.7. This switch stands apart from the many other options with its ultra-low on-resistance of 8 mΩ and its fast-switching capabilities [5].
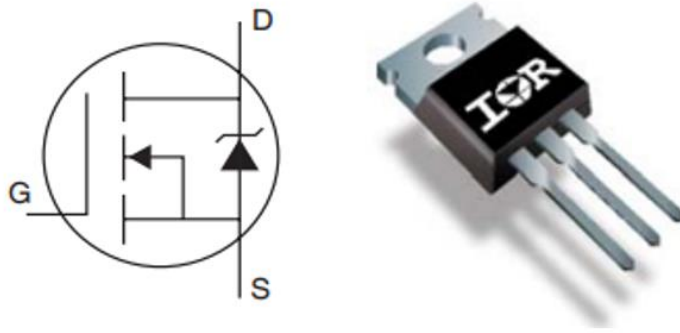
15

Figure 2.7: IRF3205 Power MOSFET (Reprinted from [5])

The 1N5817 Schottky Barrier Rectifier was selected as the diode. This diode has a low forward voltage of 450mV at 1A [6]. Given that my boost converter is expected to operate at much smaller currents than 1A, an adequately low forward voltage is expected when implemented into the final design.

The most important design parameter for my boost converter is to ensure that it operates at a maximized power transfer. By maximizing the power transfer from the TEG to the boost converter, I can maximize the energy conversion and thus the cooling effect on the system will also be maximized. Since the primary focus of this project is to mitigate the heat from the IMD battery as much as possible, maximum power point is a critical design requirement. The maximum power transfer theorem states that the maximum magnitude of power is achieved when the source impedance matches the load impedance [7]. A simplified way to visualize the interaction between the TEG and the boost converter is to draw an equivalent circuit such as the one shown in Figure 2.8.
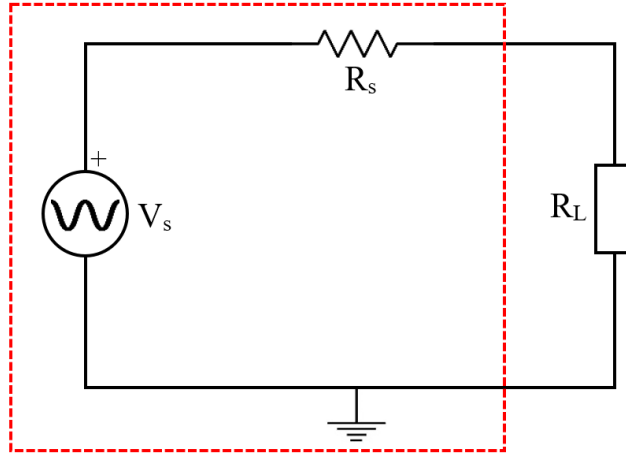
16

Figure 2.8: Simplified Equivalent Circuit Model

In the equivalent circuit, the source voltage and resistance correspond to that of the TEG and the load is the observed input impedance of the boost converter. The selected TEG has a defined source impedance of 8.3Ω with a source voltage that is dependent upon the temperature gradient [3]. This indicates that to achieve maximum power transfer, my boost converter's input/load impedance, should be designed to be 8.3Ω. At this maximum power transfer configuration, I can expect the open circuit voltage of my TEG, seen in Fig. 2.8 as V_s, to be exactly twice of value of the input voltage to the boost converter. At matched impedances, half of the voltage should drop across the TEG's source impedance which leaves the other half to drop across the boost converter.

To ensure that my boost converter is optimized for maximum power transfer, the component values will need to be adjusted to the appropriate levels. The input impedance of the boost converter can be seen as

$$R_{in} = R_L \times (1 - D)^2 \tag{2.5}$$

where R_L is the load impedance at the output of the boost converter and D is the selected duty cycle applied to the switching device. Given a fixed duty cycle, the load impedance can be selected

17

to ensure that the impedance of the boost converter matches that of the TEG. It is important to note that the duty cycle directly affects the output voltage and can be seen as

$$V_o = \frac{V_{in}}{(1 - D)} \qquad (2.6)$$

where V_{in} is the input voltage to the boost converter and D is the duty cycle selected [8]. Since a minimum of 1.5V at the output is desired from the boost converter, the duty cycle must be appropriately selected. A valid switching frequency will also dictate the converter's efficiency and functionality. Typical booster designs use a value between 100kHz to 2MHz. Increasing the frequency will reduce the inductor current ripple and the capacitance voltage but will also result in increased power loss. Lower frequencies will likely perform better for ideal power transfer and efficiency. A matched impedance will allow for a maximum power transfer and thus, a maximized cooling efficiency for my design.

2.3.2.1 Commercial Boost Converter Functional Validation

The ELC-BVB040 Bipolar Voltage Booster was not tested independently from the TEG since it had been used previously and already validated for functionality. The bipolar booster is designed to boost any input voltage of at least 40 mV up to approximately 10 V before being throttled. The booster is optimized for use with TEG's and has an integrated MPPT capability to ensure ideal power transfer. To observe the results when using the commercial boost converter, refer to the Results section of this document.

2.3.2.2 Custom Boost Converter Functional Validation

The selected custom boost converter design was first tested in simulations before being constructed and tested. The boost converter was designed in Multisim with the following component values:

- Inductor: 1 mH

- VTEG (open circuit TEG voltage): 300mV

- Capacitor: 100 µF

- Ro (Load resistor): 1750 Ω

- Switching Frequency: 10kHz

- Duty Cycle: 93%

The simulated boost converter design in Figure 2.9 was then tested to ensure maximum power transfer and sufficient boosting at the output.
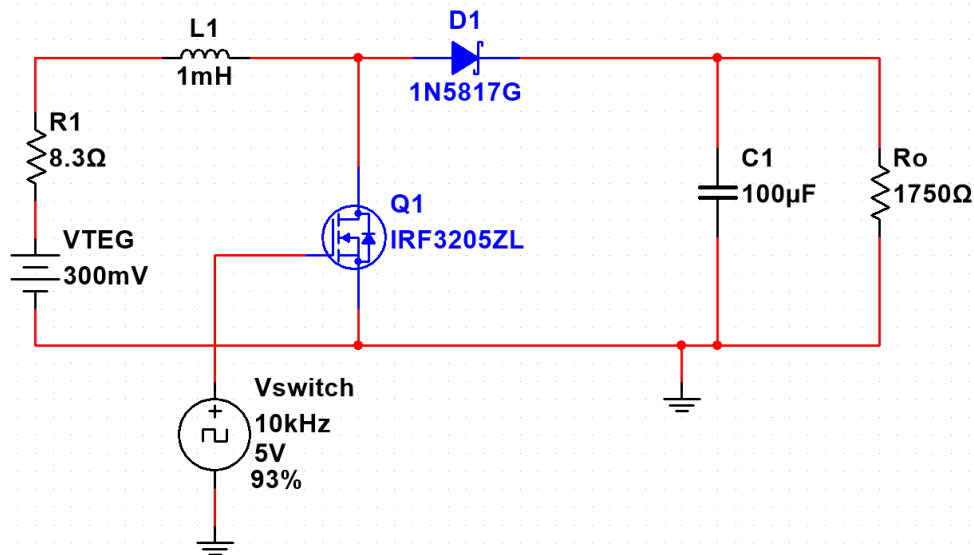

Figure 2.9: Simulated Boost Converter Design Schematic

From Figure 2.10, the simulations showed an average input voltage to the boost converter of about 151.34 mV and a boosted output voltage of 2.04 V. These results were observed while using an open circuit voltage of 300 mV. The input voltage transient output looks thick because of the oscillation induced by the inductor. The only relevant parameter for power transfer is the average DC input voltage.
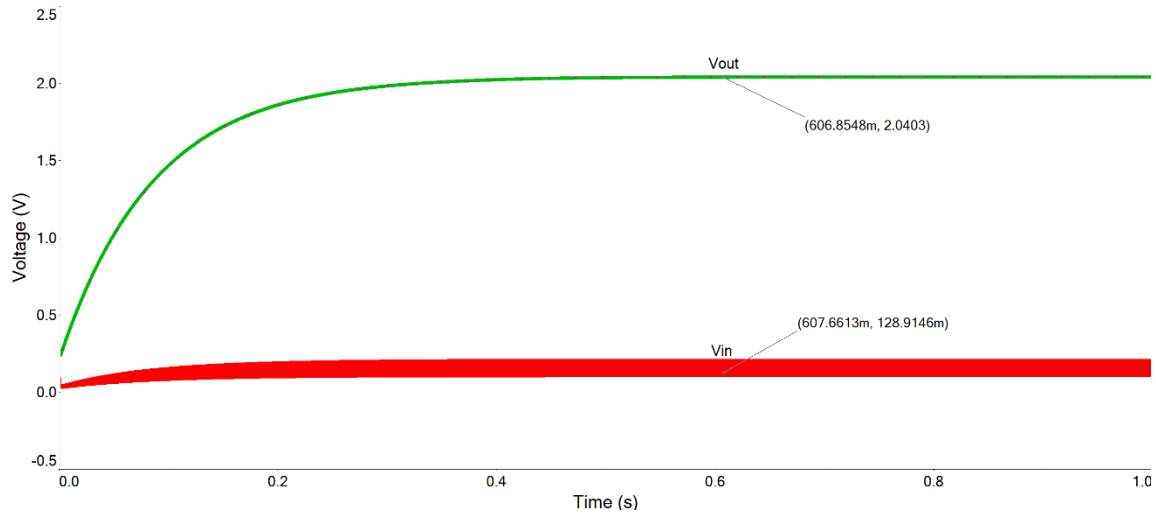
Figure 2.10: Simulated Boost Converter Transient Plot

The simulated circuit was able to boost to a sufficiently high output voltage and more importantly, the power transfer was maximized. The power transfer can be calculated by observing the input voltage as shown below

$$PT = 1 - \frac{|V_{in,ideal} - V_{in,actual}|}{V_{in,ideal}} = 1 - \frac{|150 - 151.34|}{150} = 99.1\% \qquad (2.7)$$

where $V_{in,\,ideal}$ is the ideal input voltage when at maximum power transfer and $V_{in,\,actual}$ is the observed input voltage to the circuit. Maximum power theorem dictates that the ideal input voltage to the boost converter should be half the value of the TEG open circuit voltage. Any power transfer above 90% will satisfy the requirements for the boost converter. Now that the simulated circuit was working, the next step was the test the design using real components.

After some preliminary tests, the physical circuit had to be adjusted slightly to ensure sufficient power transfer. In particular, the load impedance was adjusted to 2.15 kΩ and a 10 Ω source impedance was used. Additionally, the analog discovery that provided the test input could supply a minimum of 500 mV. Thus, an open circuit of 500 mV was used instead of the 300 mV from simulations. Since my TEGs have a source impedance of 8.3 ohms, my boost converter

20

will need to be further adjusted during final testing of my design. The boost converter, shown in Figure 2.11, was tested for functionality by observing the power transfer and output voltage. The transient test, shown in Figure 2.12, showed a peak output voltage of ~1.5V and an input voltage of about 255 mV.
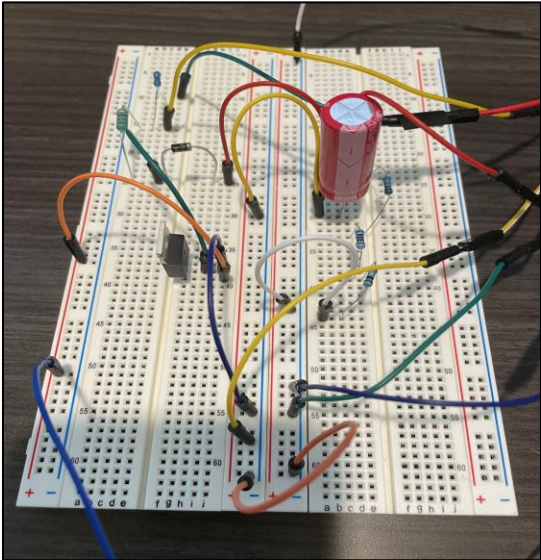

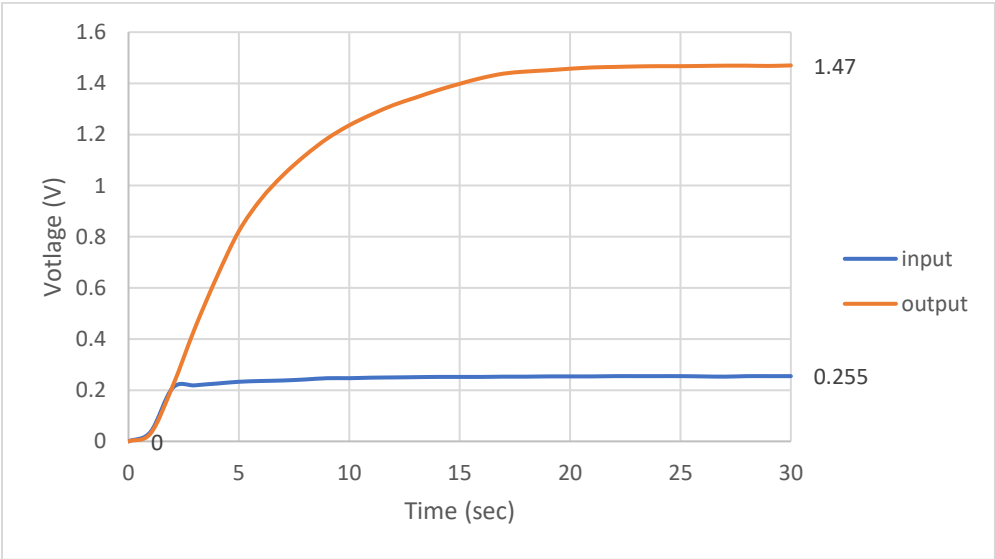*Figure 2.11: Custom boost converter circuit*

Figure 2.12: Custom boost converter performance test

After analyzing the transient plot of the physical boost converter design, the power transfer was calculated as

$$PT = 1 - \frac{|V_{in,ideal} - V_{in,actual}|}{V_{in,ideal}} = 1 - \frac{|250 - 255|}{250} = 98\% \qquad (2.8)$$

where $V_{in,\,ideal}$ is the ideal input voltage when at maximum power transfer and $V_{in,\,actual}$ is the observed input voltage to the circuit. Though the output voltage was lower in the physical circuit, this can be further enhanced during final testing by adjusting the component values. While a sufficiently high output voltage will prove that the electrical energy can be used, it is not the main objective of this research. Ensuring maximum power transfer is what will affect the cooling potential of the design and thus, it is of the highest priority in the boost converter design process. The positive test results in both simulation and physical testing confirms the functionality of the customized boost converter design.

2.3.3 Heating Element

The limiting factor affecting the charging rates for IMD devices is the heat buildup from the battery. The heating element being used is an adjustable hotplate, shown in Figure 2.13 .This will substitute and act as the battery that would begin emitting heat energy during a typical IMD charging cycle. This can be directly connected to the TEG devices to simulate heat transfer from an IMD battery. The FDA limits an implantable device's temperature to a maximum of 5°C above the human body temperature. The testing environment for my design will be the ambient room temperature. Using the room temperature to represent the body temperature that an IMD is exposed to, the maximum hotplate temperature must be set at 5°C above the room temperature.

Figure 2.13: Heating Element Selected for Testing

2.3.3.1 Heating Element Functional Validation

For testing purposes, the most important function of the heating element is its ability to reach a specified temperature. To validate the functionality and accuracy, the hotplate was set to 46°C and a thermocouple was placed on the plate. The thermocouple verified that the hotplate was functioning properly and was sufficiently accurate within 0.3°C. A screenshot of the functional test is shown in Figure 2.14.

Figure 2.14: Heating Element Functional Test

2.3.4 Measurement Equipment

To measure the success of my design, the boost converter's output voltage and power transfer need to be measured. Additionally, the temperatures at the cold face of the active TEG and an inactive TEG need to be recorded. To record temperature data, the TC0520 digital thermocouple depicted in Figure 2.14 will be utilized. It is capable of recording four temperature readings simultaneously and logging them using the Windows-compatible software that is provided.

An Analog Discovery 2, shown in Figure 2.15, will be used to record the input and output DC voltages of the boost converter during testing. The AD2 will also provide the pulse input wave to the boost converter's switching device.

Figure 2.15: Analog Discovery 2 Measurement Tool (Reprinted from [9])

2.3.5 Body-Representative Medium

Since this project involves technology being implanted in human patients, the design should, ideally, be tested in an enclosed environment. The hot face of the TEG is already "enclosed" since the entire TEG face is in contact with the heating element. The external (cold) face of the TEG, however, is exposed to the ambient environment. Since air does not share a similar thermal conductivity as the human body, a material such as water is preferred. The thermal conductivity of air at 25°C is approximately 26.24 mW/m K as compared to water which is at 607 mW/m K. Thermal conductivity of human tissue is approximated between 290 and 1060 mW/m

24

K. Air does not have a sufficiently high thermal conductivity to match the conditions that an IMD operates in.

To replicate the IMD operation conditions, the external TEG face will be exposed to a body of water at room temperature. Since the TEG can only convert a small percentage of the total heat energy applied, the unconverted thermal energy will slowly make its way to the cold face of the TEG. The water that will be used to replicate the body will slowly be exposed to that heat and rise in temperature. The water that is connected to the active TEG is expected to increase at a slower rate than the water connected to the inactive TEG. This will prove that a TEG design configured for maximum power transfer can cool the system by converting a portion of thermal energy into electrical energy.

2.4   Experimental Setup

To measure the success of my design two TEGs were mounted to the hotplate simultaneously, one inactive and one active. The inactive TEG is left in an open circuit configuration, not transferring any power. This will serve as benchmark to compare the active TEG against. The active TEG is the TEG connected to the power harvesting circuit (boost converter). With the active TEG delivering maximum power to the boost converter, the TEG will be converting as much energy as possible. This will maximize the cooling potential which can be defined from the comparison to the inactive TEG. The active TEG's cold face increase in temperature at a slower rate than the inactive TEG.

Additionally, voltage and temperature data will be recorded to measure the overall impact made by a TEG at maximum power transfer. A thermocouple data logger will be used to measure temperature data and an AD2 will be used to observe input and output voltages. The experimental setup depicted in Figure 2.16 below.
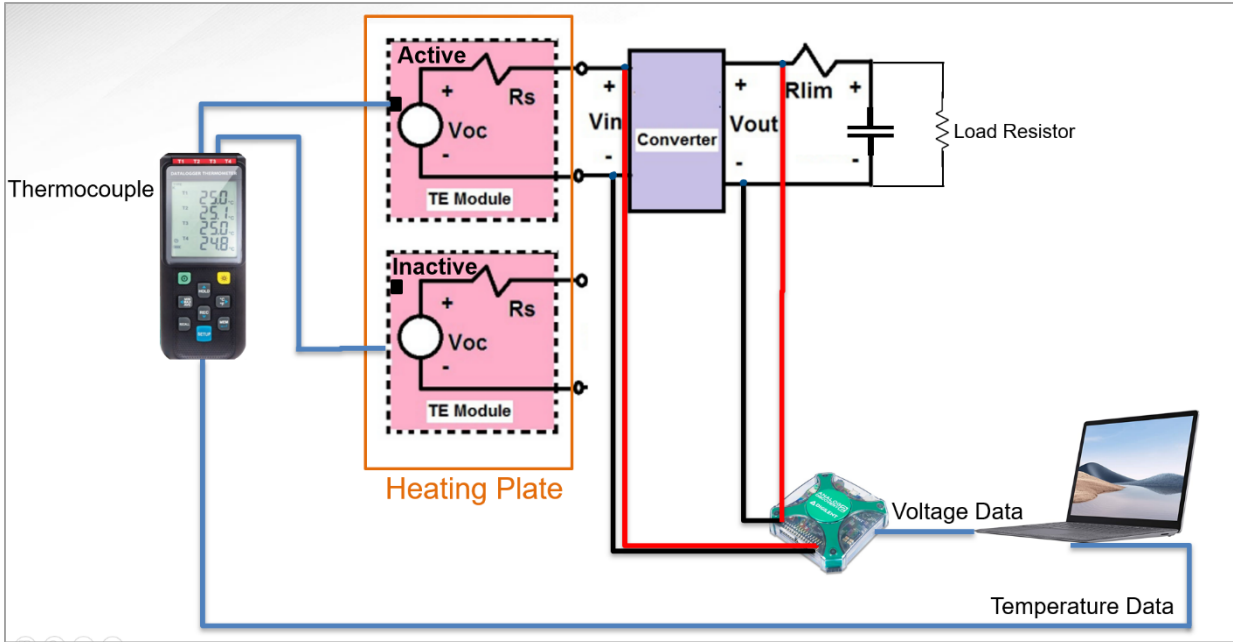
Figure 2.16: Diagram of Experimental Setup

3.   RESULTS

3.1   Operational Overview

The first phase of the research utilized the commercial bootstrap boost converter and did not emphasize the enclosed environment that IMD's operate in. The TEG's in the first phase of testing were left exposed to the ambient environment and the cooling capability of the system was measured. In the second phase, a customized boost converter was designed and tested used discrete components. The commercial booster from phase one was replaced with the custom design and the phase one experiments were repeated with the new design. One important change in phase two is that the TEG's were isolated from the ambient environment by using water as a medium to represent the human body. This more accurately represents a typical IMD operating environment where the device is isolated from the external environment. Voltage and temperature readings were recorded in both phases to observe the impacts that each of the designs had on the thermal output of the system.

3.2   Phase 1 Initial Results

In the first phase of testing, I started by setting up the experiment as discussed in section 2.4 of this document. A copper plate was used between the hotplate and the TEG's to allow for both TEG's to fit entirely. Thermocouple leads were taped to the TEG cold face with a small amount of thermal paste applied to ensure accurate temperature readings. The hotplate was set to 30 °C to provide a ΔT of 5 °C from the observed room temperature at about 25 °C. Additionally, a 4700 μF capacitor was used for charging at the output of the boost converter. One critical factor to note is that, in this first experiment, the TEG's were mounted prior to the activation and heating of the hotplate. The setup can be seen below in Figure 3.1
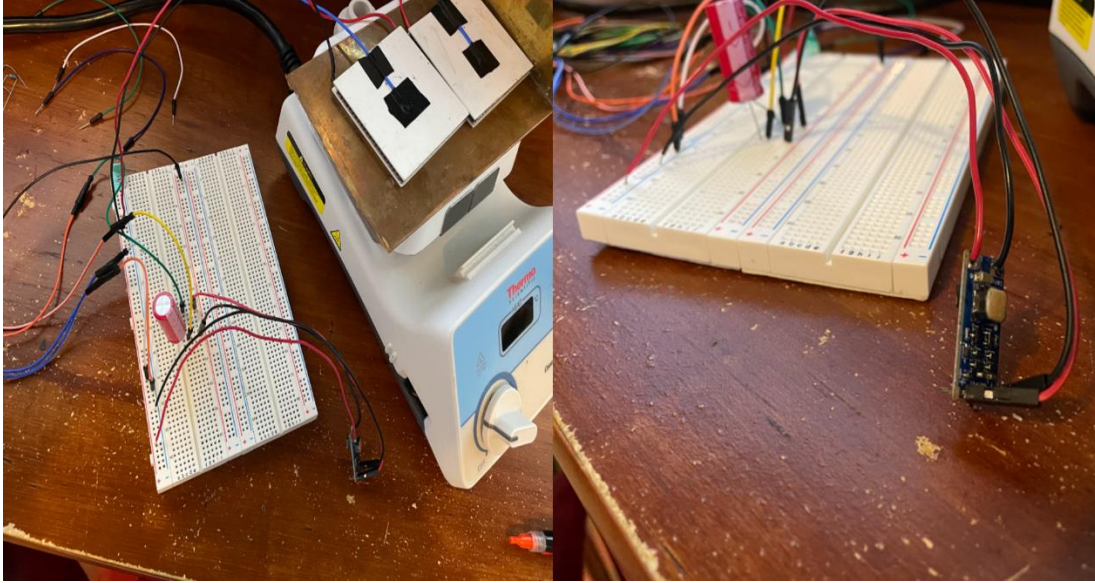
Figure 3.1: Image of First Experimental Setup

The first test was initiated by activating the AD2 and starting the thermocouple's data logging software. Then the hotplate was set to 30°C. The temperature readings of both the active and inactive TEGs are shown in Figure 3.2 below.
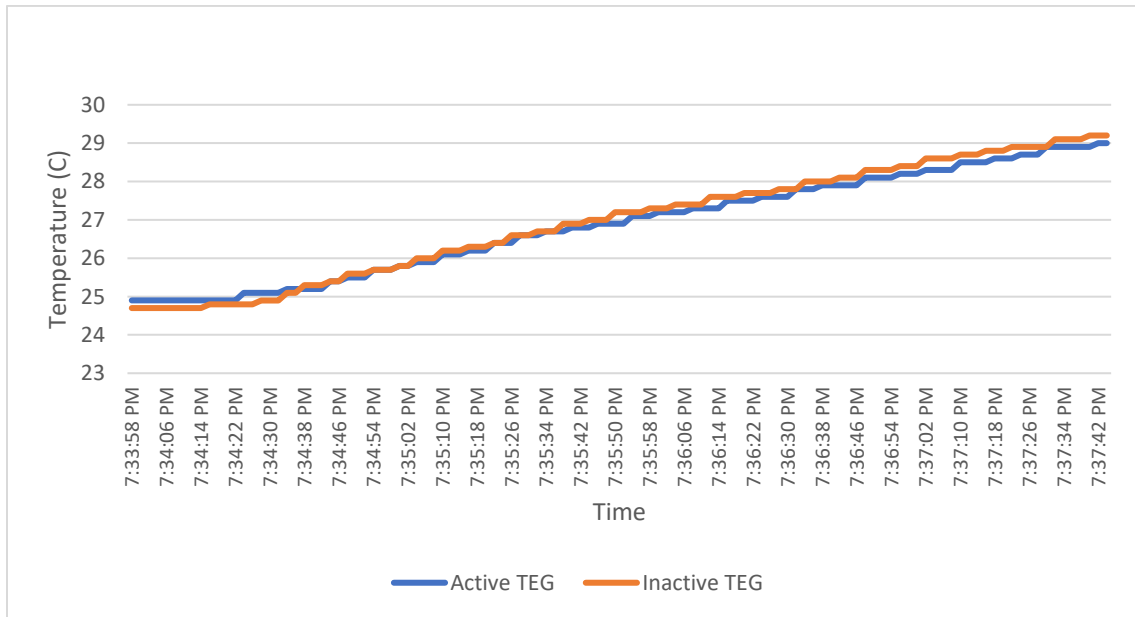

Figure 3.2: Phase One Initial Temperature Measurements

The temperature results showed the Active TEG increasing at a slightly smaller rate than the inactive TEG which was some indication of cooling. Comparing the slopes of each of the TEG's, it was determined that the active TEG heated up at .0195 C°/sec and the inactive TEG at .0214 C°/sec. Taking the different yields an effective cooling rate by the active TEG of .114 C°/min. This yields a noticeable cooling rate; however, this does not reflect measurable cooling on a scale that is desired or useful. The voltage measurements in Figure 3.3 revealed a problem with the boost converter.
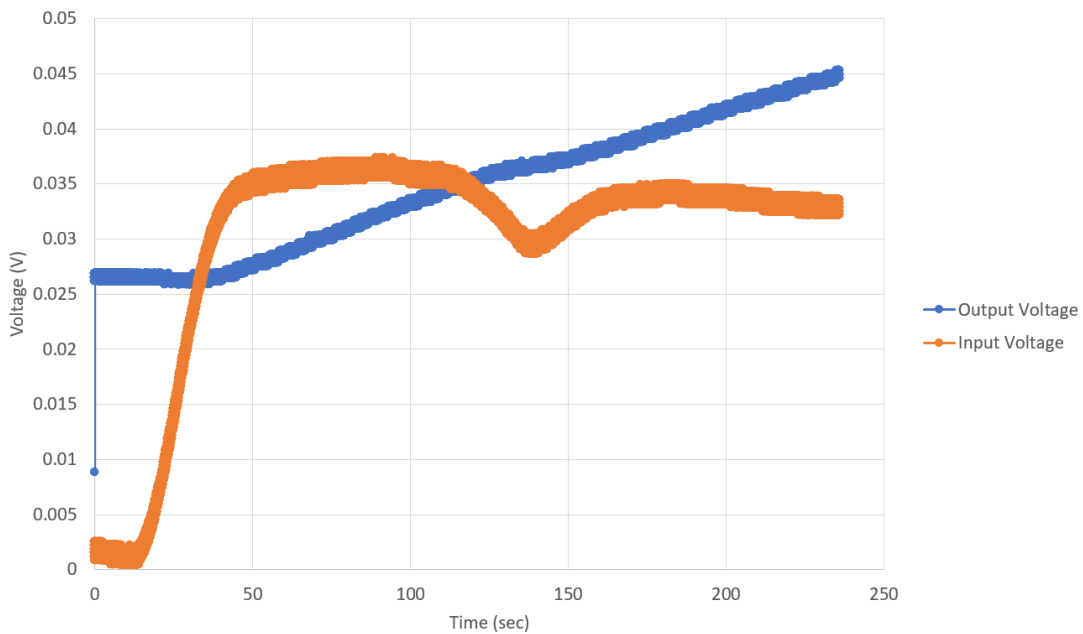

Figure 3.3: Phase One Initial Voltage Measurements

This is where Experiment 1 fails to meet some requirements. The first observation is that the maximum input voltage does not reach the minimum requirement of 40 mV which is the minimum activation voltage for the ELC-BVB040 bipolar converter. The boost converter did not have sufficient input voltage to adequately begin boosting the voltage. Thus, the output was scarcely boosted and did not meet the 1.5 V minimum specification. This indicates that the TEG

did not have a sufficient temperature gradient to provide the adequate input voltage. From these initial results, it was apparent that the testing conditions would need to be adjusted.

The maximum ΔT across the TEG was observed to be 0.651 °C which is much lower than the expected value closer to 5 °C. From this, I theorized that the cold face of the TEG was heating up much quicker than expected which closed the temperature gap and resulted in a lower voltage. This is almost certainly because the air that the TEG was exposed to did not dissipate the heat in the same way that a medium such as water would. Since the use of an enclosed environment was only emphasized in the second phase of the research, the temporary solution was to momentarily remove the TEGs from the hotplate. This allows the hotplate heat up before exposing the TEGs and allows for a greater ΔT. In the final stage one tests, I account for this issue and re-run the experiment.

3.3   Phase 1 Final Results

After the failed results from my first experiment, I learned that I would need to ensure a greater temperature gradient across the TEG's without exceeding the ~30°C maximum (assuming room temperature of 25°C). The primary changes made to my setup as compared to the first setup are the following:

- Reduced charging capacitor from large 4700uF to 100uF

- Removed Copper plate

- Mounted the TEG's after letting the hotplate heat up for one minute.

The new setup is shown in Figure 3.4. This adjusted design was initiated by first setting the hotplate to 30°C with the TEG's not yet mounted to the hotplate. Next, the AD2 and thermocouple's data logging software were activated. The two TEGs were then placed onto the

30

hotplate at the same time after letting the hotplate heat up for at least one minute. The resulting

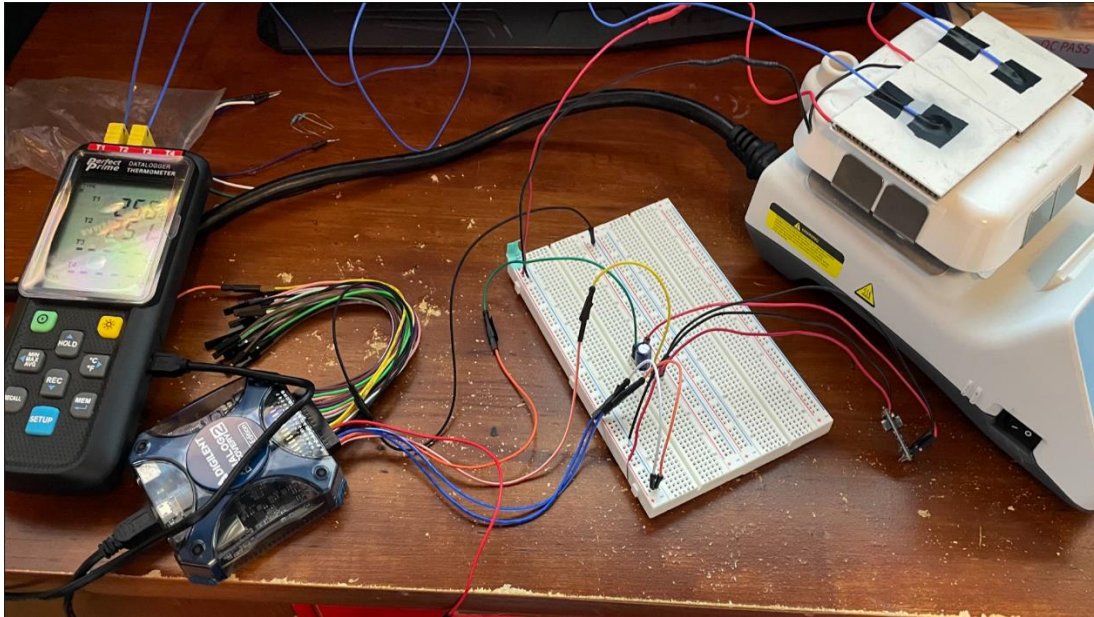temperature readings at the cold sides of the active and inactive TEGs are shown in Figure 3.5.

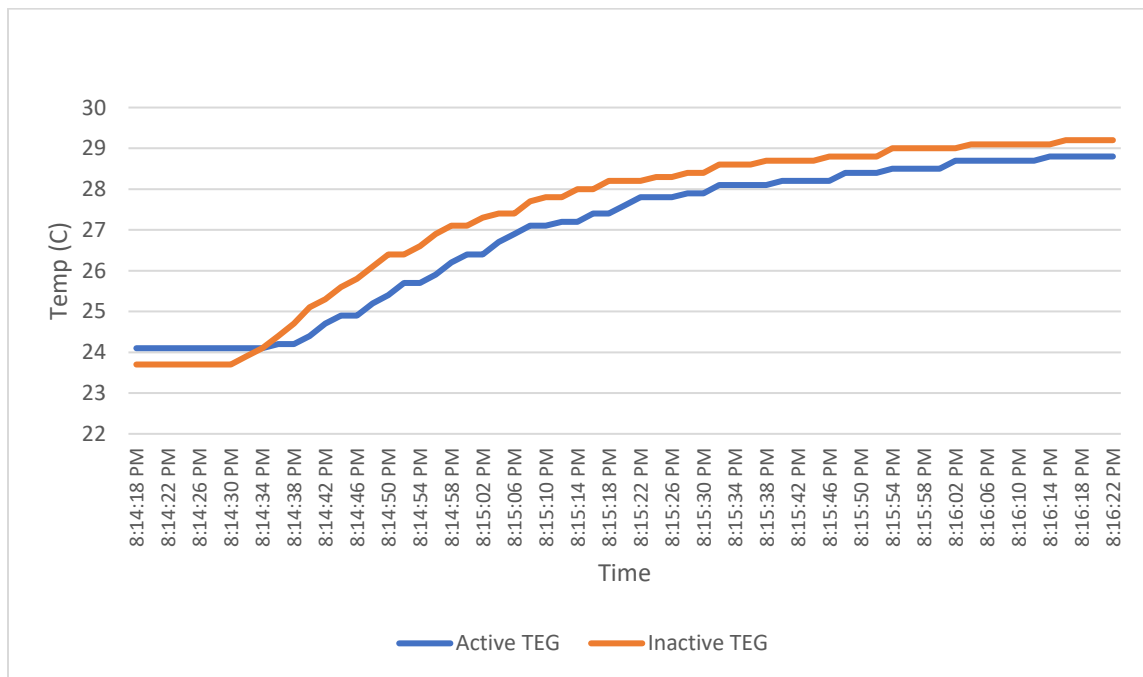*Figure 3.4: Image of Second Experimental Setup*

Figure 3.5: Phase One Final Temperature Measurements

The temperature results indicated the active TEG's cold face increasing in temperature at a slower rate compared to the inactive TEG. Like the first experiment, this proves that the active TEG is reducing the heating rate experienced by the body. After comparing the peak slopes seen at the beginning, an active TEG heating rate of .0704 C°/sec and an inactive TEG heating rate of .0977 C°/sec were observed. Taking the difference yields an effective cooling rate of 1.636 C°/min. This much larger than in the first experiment, likely due to the increased TEG efficiency operating at greater temperature gradients. More importantly, the boost converter was provided sufficient voltage to activate as depicted in Figure 3.6.
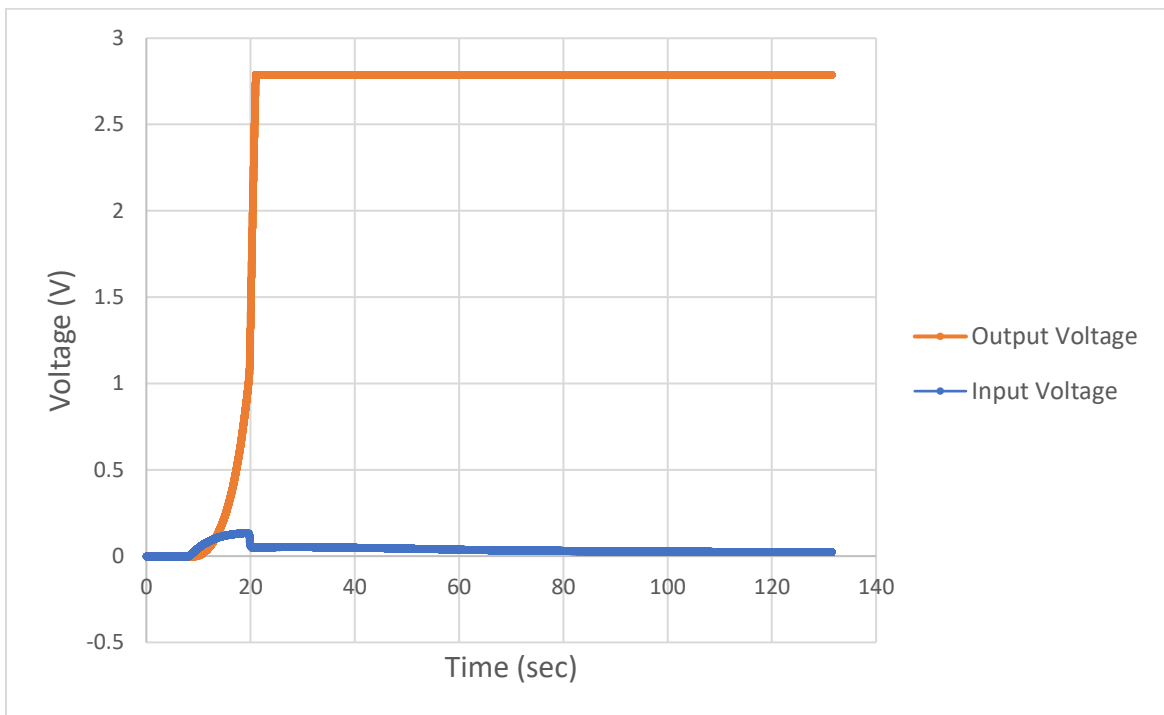

Figure 3.6: Phase One Final Voltage Measurements

The measured voltages at the input and output of the boost converter immediately look much better than the measurements from the first setup. The input grew to a maximum of 135mV which meets the 40mV requirement of the booster. This was sufficient to activate the boost

converter which managed charge the 100uF capacitor up to 2.78V. This also exceeds my output voltage goal of 1.5V.

I did not have temperature probes to also capture the ΔT across the TEG. To determine the actual ΔT across the TEGs and the power transfer, the boost converter voltage curves within the data sheet were used, shown in Figure 3.7. The voltage curves and the known power transfer equations allow for accurate calculation of the power transfer.
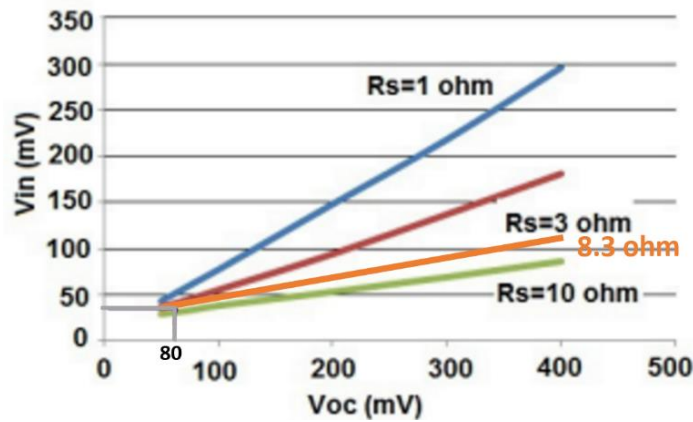

Figure 3.7: Vin to Voc Curves for VB0410 Boost Converter (Referenced from [2])

The corresponding V_{oc} for the known $V_{in, max}$ of 135 mV is estimated to be ~500 mV. The corresponding V_{oc} for the known $V_{in, avg}$ of 38.5 mV is estimated to be ~80 mV. Re-arranging equation 2.1 the ΔT can be solved for as shown below:

$$\Delta T = \frac{V_{oc}}{j \times S} = \frac{500 \; mV}{(576)(200 \times 10^{-6})} = 4.34°C \tag{3.1}$$

where S is the Seebeck coefficient and j is the number of series connected thermo elements. At maximum power transfer Vin = ½ V_{oc} . Thus, at $V_{oc, max}$ of 500 mV, the Vin should be at 250 mV for maximum power transfer (MPPT). At $V_{oc, avg}$ of 80mV, Vin should be 40mV for MPPT. The observed $V_{in, max}$ and $V_{in, avg}$ were 135 mV and 38.5 mV, respectively. The power transfer can then be calculated as shown below.

33

$$PT \text{ } at \text{ } V_{in,max} = \frac{V_{in,observed}}{V_{in,ideal}} = \frac{135 \text{ } mV}{250 \text{ } mV} = 54\% \qquad (3.2)$$

$$PT \text{ } at \text{ } V_{in,avg} = \frac{V_{in,observed}}{V_{in,ideal}} = \frac{38.5 \text{ } mV}{40 \text{ } mV} = 96.25\% \qquad (3.3)$$

This confirms that the average power transfer of the boost converter throughout the test was sufficiently high (within 10% of maximum power transfer). To summarize, this second experiment indicates than when operating within 3.75% of maximum power transfer, my design cooled the system by about 1.363 deg/min. More accurate cooling capabilities may be seen in the second phase of testing due to the implementation of a medium of water at the TEG cold side. The use of water will better reflect and IMD's true operating conditions and allow for more efficient heat dissipation.

3.4   Phase 2 Final Results

In the second phase of testing, I started by setting up the experiment similarly to the phase 1 setup. A copper plate was used between the hotplate and the TEG's to allow for both TEG's to fit entirely. Thermocouple leads were taped to the TEG cold face with a small amount of thermal paste applied to ensure accurate temperature readings. The noteworthy changes made in phase 2 include the use of a custom-built boost converter and the use of water to isolate the system. Water has similar thermal properties to the human body and thus, it is an excellent medium to use for experimentation. Additionally, tin foil was wrapped around the sides of the copper plate such that the TEG's maintained direct contact while the bags of water were kept separate from the hot plate. This was done to ensure accuracy during testing and can be seen in Figure 3.8. After preliminary tests with the integrated system, some of the component values in the boost converter were adjusted to optimize performance. The final boost converter component values chosen were the following:

- Inductor: 680 μH

- Capacitor: 4700 μF

- Ro (Load resistor): 2000 Ω

- Switching Frequency: 10kHz

- Duty Cycle: 95%

The selected design parameters allowed for a greater boost voltage while maintaining a closely matched impedance to the TEG.
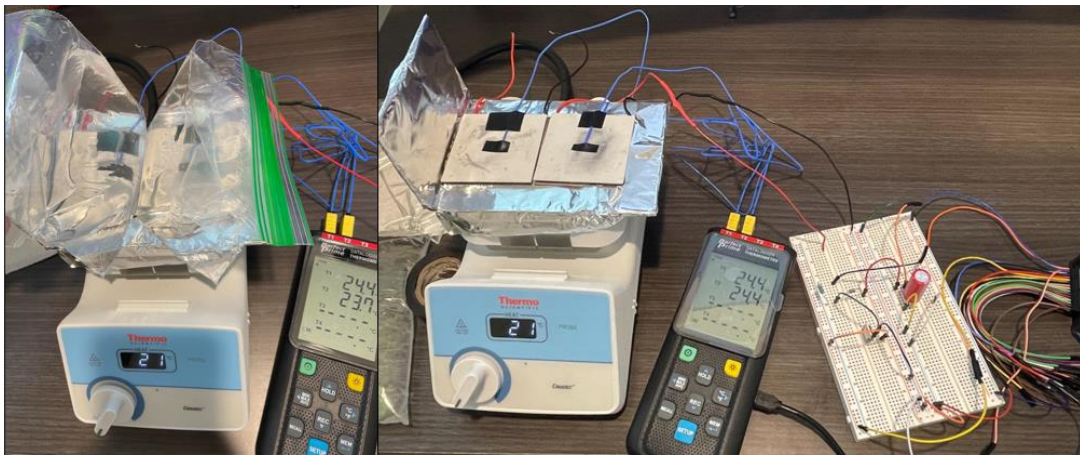

Figure 3.8: Image of Final Experimental Setup

The final validation tests were initiated by first activating the AD2 and starting the thermocouple's data logging software. Then the hotplate was set to 28°C. The temperature readings of both the active and inactive TEGs are shown in Figure 3.9.
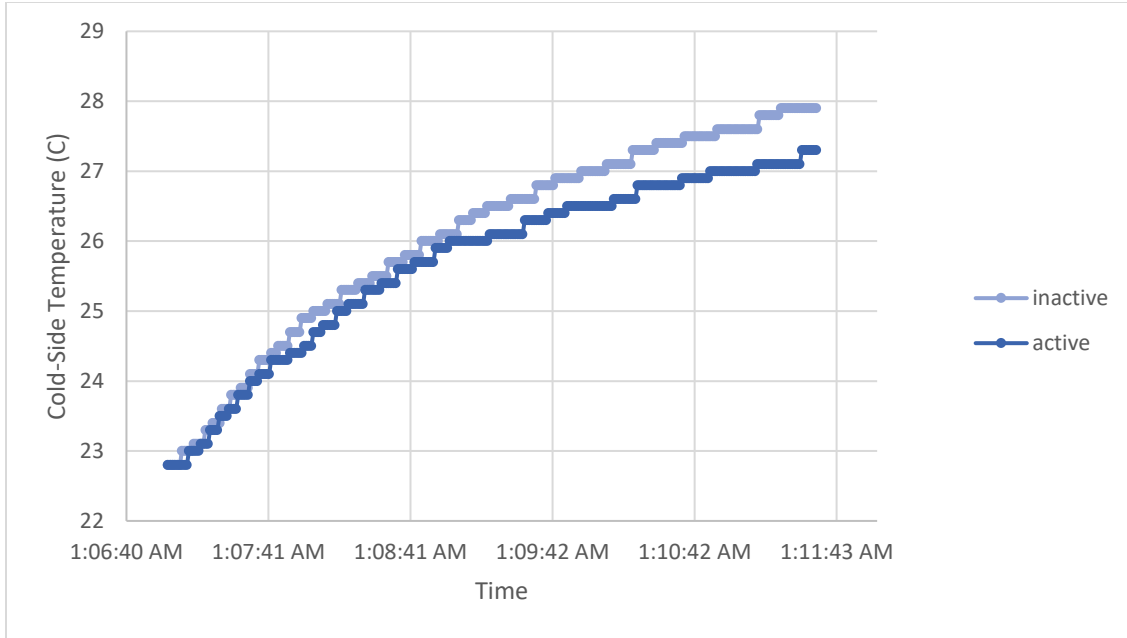
Figure 3.9: Phase Two Final Temperature Measurements

The temperature results depicted in Figure 3.9 showed the Active TEG increasing at a smaller rate than the inactive TEG which is indicative of cooling. The peak cooling rate was found by looking at the temperature readings during the last few minutes. The average cooling rate was found by comparing the temperature readings during the entire experiment. The average cooling rate and peak cooling rate were calculated as 0.115 C°/min and 0.196 C°/min, respectively.

$$Avg\ Inactive\ Heating\ Rate = \frac{\Delta T_{total}}{\Delta Time} = \frac{(27.9 - 22.8)}{314\ sec} = 0.01624\ \frac{C°}{sec} \qquad (3.4)$$

$$Avg\ Active\ Heating\ Rate = \frac{\Delta T_{total}}{\Delta Time} = \frac{(27.3 - 22.8)}{314\ sec} = 0.014\ \frac{C°}{sec} \qquad (3.5)$$

$$Avg\ Cooling\ Rate = (0.01624 - 0.014) \times 60 = 0.115\ \frac{C°}{min} \qquad (3.6)$$

$$Peak\ Inactive\ Heating\ Rate = \frac{\Delta T_{last\ 153\ sec}}{\Delta Time} = \frac{(27.9 - 26.1)}{153\ sec} = 0.0117\ \frac{C°}{sec} \qquad (3.7)$$

$$Peak\ Active\ Heating\ Rate = \frac{\Delta T_{last\ 153\ sec}}{\Delta Time} = \frac{(27.3 - 26)}{153\ sec} = 0.0085\ \frac{C^\circ}{sec} \qquad (3.8)$$

$$Peak\ Cooling\ Rate = (0.0117 - 0.0085) \times 60 = 0.196\ \frac{C^\circ}{min} \qquad (3.9)$$

The voltage measurements at the input and the output of the boost converter were also measured during the final experiment and are depicted in Figure 3.10. The boost converter saw a peak input voltage of approximately 254 mV and boosted to a peak output voltage of approximately 1.43 V. Though my aim was an output voltage of 1.5 V or greater, the observed output of 1.43 V is a perfectly acceptable boosted voltage that is suitable for many applications.
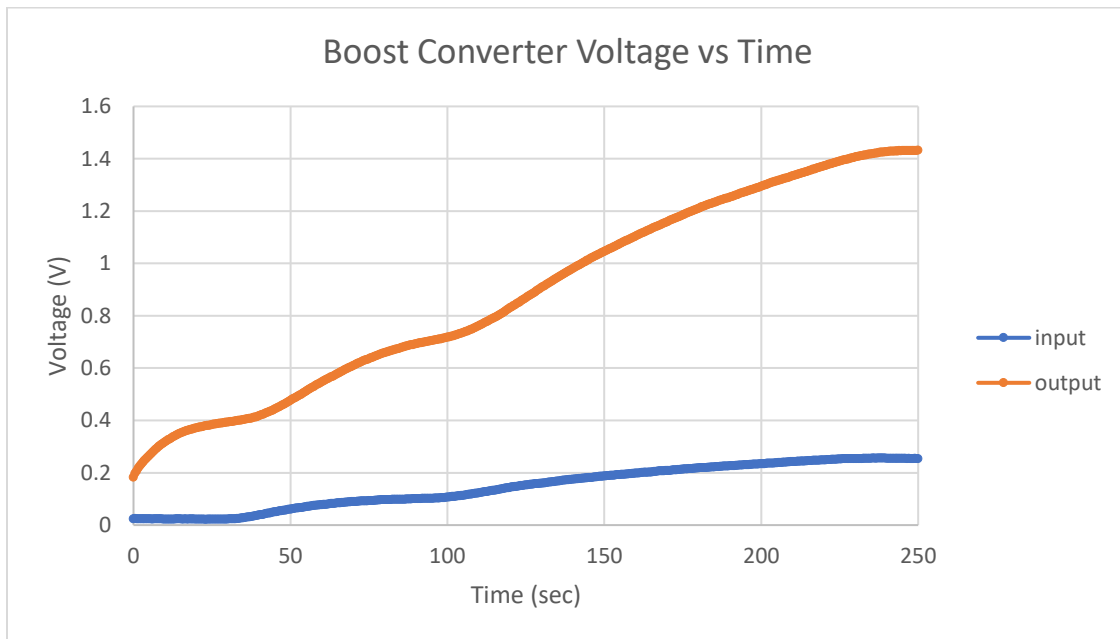

Figure 3.10: Phase Two Final Voltage Measurements

The maximum temperature gradient that was observed across the active TEG was 4.6°C where the hot face of the TEG was at 27.4°C and the cold face was at 22.8°C . Figure 3.11 shows a screenshot of the maximum temperature gradient taken during testing.

Figure 3.11: Maximum ΔT Observed during Phase Two

Using the peak temperature gradient seen across the active TEG, I used the known TEG relationship from Equation 2.3 to determine the open circuit voltage. The open circuit voltage at a ΔT of 4.6°C was determined to be 538 mV. Additionally, the peak input voltage to the boost converter was seen as 253.6 mV. Knowing that the input voltage should be exactly half of V_{oc} for maximum power transfer, the input voltage should ideally be 269 mV. Comparing the ideal input voltage to the observed input voltage, the power transfer is calculated as 94%. This meets my goal of a 90% or greater power transfer which is critical in maximizing the resulting cooling effects on the system.

$$PT\ at\ V_{in,max} = \frac{V_{in,observed}}{V_{in,ideal}} = \frac{253.6\ mV}{269\ mV} = 94\% \tag{3.10}$$

4. CONCLUSION

The goal of the performed research was to establish that thermoelectric properties can be implemented to ultimately reduce the charging times of commercially used implantable medical devices. The core challenge that must be addressed to enable faster charging is to minimize the heat buildup from the device's battery during the charging process. To accomplish this, as much energy as possible needs to be harvested and converted from thermal and into electrical energy. This allows for greater current throughput during charging while also meeting FDA health regulations on IMD's. By maximizing the cooling potential of my thermoelectric system, I can determine how effective these devices might be if implemented in commercial products.

After comparing the temperature flow across an active and inactive TEG, I observed TEGs, when setup for optimal power transfer, can reduce the heat buildup of an IMDs battery. Both the first and second phase setups had, respectively, 96% and 94% power transfer which are sufficient to ensure optimal cooling results. The first phase of the research saw a peak cooling rate 1.636 °C/min however, this was not tested in an enclosed environment with similar thermal characteristics as the human body. In the final experiments conducted, with the incorporation of water as an insulation medium, a peak cooling rate of 0.196 °C/min was observed. While the final results yield a smaller cooling rate when compared to the results from the first phase, the second phase test is a more reliable test to look at given the implementation of an enclosed environment. Since the human body shares many characteristics of water, the second phase testing provided a much more accurate testing environment for the TEG setup.

While these tests show that thermoelectric devices can be used to noticeably reduce heat buildup in an enclosed IMD environment, there are many limitations of TEGs. Firstly, the more

thermocouples that a TEG has, the more effective it is at converting between thermal and electrical energy. Due to the small form factor of actual IMDs, the large TEG devices used in these tests could not be implemented. Thus, it is likely that TEGs would be less effective at cooling when using smaller TEG devices that are suitable for IMD integration. Additionally, TEGs have a conversion efficiency that is limited between 5% to 15% [10]. The temperature gradient has a significant impact on the resulting conversion efficiency of such devices. FDA regulations limit the temperature difference to about 5°C which is an extremely small temperature gradient to work with. When using smaller TEG devices, smaller output voltages will be achievable. This ultimately limits the energy harvesting efficiency of the system and will result in further reduced cooling capabilities of such a system. These factors should be considered when utilizing thermoelectric properties to cool within an enclosed environment such an implantable medical device.

REFERENCES

[1]   J. Richard and J. Richard, "How to build a homemade thermoelectric generator," *Top Magnetic Generator*, 13-Mar-2021. [Online]. Available: https://topmagneticgenerator.com/build-homemade-thermoelectric-generator/.

[2]   "ELC-BVB040 Bipolar Voltage booster 40MV," *Custom Thermoelectric*. [Online]. Available: https://customthermoelectric.com/elc-bvb040-bipolar-voltage-booster-40mv.html.

[3]   "TXL-287-03z teg 62 x 62mm," *Custom Thermoelectric*. [Online]. Available: https://customthermoelectric.com/txl-287-03z-teg-62-x-62mm.html.

[4]   "Boost Converters," *Learnabout Electronics*, Dec-2020. [Online]. Available: https://learnabout-electronics.org/PSU/psu32.php#:~:text=The%20boost%20converter%20is%20different,available%20output%20current%20must%20decrease.

[5]   International Recifier, "IRF3205PBF product data sheet - infineon technologies," *infineon*. [Online]. Available: https://www.infineon.com/dgdl/Infineon-IRF3205-DataSheet-v01_01-EN.pdf?fileId=5546d462533600a4015355def244190a.

[6]   Diodes Incorporated, "1.0A Schottky Barrier Rectifier," *diodes*. [Online]. Available: https://www.diodes.com/assets/Datasheets/ds23001.pdf.

[7]   B. Dull, "Understanding the maximum power theorem," *Triad Magnetics*, 10-Apr-2018. [Online]. Available: https://info.triadmagnetics.com/blog/maximum-power-theorem.

[8]   B. Hauke, "Basic calculation of a boost converter's power stage," *Texas Instruments*, 2014. [Online]. Available: https://www.ti.com/lit/an/slva372c/slva372c.pdf.

[9]   S. K, "Analog discovery 2," *Analog Discovery 2 - Digilent Reference*. [Online]. Available: https://digilent.com/reference/test-and-measurement/analog-discovery-2/start.

[10]   D. Enescu, "Chapter: Thermoelectric Energy Harvesting: Basic principles and applications," *IntechOpen*, 21-Jan-2019. [Online]. Available: https://www.intechopen.com/chapters/65239.